Coding principles of the canonical cortical microcircuit in the avian brain

Ana Calabrese[a] and Sarah M. N. Woolley[a,b,c,1]

[a]Program in Neurobiology and Behavior, [b]Psychology Department, and [c]Kavli Institute, Columbia University, New York, NY 10027

Edited by Harvey Karten, University of California, San Diego, La Jolla, CA, and accepted by the Editorial Board January 20, 2015 (received for review May 8, 2014)

Mammalian neocortex is characterized by a layered architecture and a common or "canonical" microcircuit governing information flow among layers. This microcircuit is thought to underlie the computations required for complex behavior. Despite the absence of a six-layered cortex, birds are capable of complex cognition and behavior. In addition, the avian auditory pallium is composed of adjacent information-processing regions with genetically identified neuron types and projections among regions comparable with those found in the neocortex. Here, we show that the avian auditory pallium exhibits the same information-processing principles that define the canonical cortical microcircuit, long thought to have evolved only in mammals. These results suggest that the canonical cortical microcircuit evolved in a common ancestor of mammals and birds and provide a physiological explanation for the evolution of neural processes that give rise to complex behavior in the absence of cortical lamination.

functional connectivity | cortex evolution | songbird | sensory coding

The cognitive abilities of birds suggest that the avian brain contains sophisticated information-processing circuitry. Recent studies have demonstrated that corvids, such as crows, rooks, and jays, exhibit innovative tool manufacture (1), referential gesturing (2), causal reasoning (3, 4), mirror self-recognition (5), and planning for future needs using recent experience (6). Other birds can perform complex pattern recognition (7), long-term recollection (8), and numerical discrimination (9), paralleling the performance of primates. Songbirds, such as zebra finches (*Taeniopygia guttata*, the species studied here), learn to produce and recognize complex vocalizations for social communication, with numerous parallels to speech learning and perception (10).

Although cognitive skills in birds and nonhuman mammals are often comparable, avian and mammalian palliums exhibit very different anatomical organization. Although the organization of ascending sensory pathways and subpallial structures are similar in avian and mammalian brains (11), the avian pallium (referred to hereafter as the cortex) lacks the distinctive six-layered structure of the mammalian neocortex (12). Instead of a laminar structure, the avian cortex is composed of interconnected nuclei and bands of neurons that form distinct processing regions. The avian primary auditory cortex (avian A1) is organized into adjacent processing regions, collectively called the field L/CM (caudal mesopallium) complex, that are stacked in a dorsorostral to ventrocaudal orientation (13, 14) (Fig. 1 and Fig. S1). Regions of avian A1 are delineated by differences in cytoarchitecture and connectivity (13, 15) (*SI Materials and Methods*) and are organized into superficial (field L1 and lateral caudal mesopallium, CML), intermediate (field L2a and -b), and deep (field L3) regions, similar to neocortical layers. A posterior region, the caudal nidopallium (NC) is referred to as "secondary" cortex here. Fig. 2*A* shows a schematic diagram of the main connections among regions (modified from ref. 16).

Despite large-scale differences in the organization of the avian cortex and mammalian neocortex, similarities in these brain areas have recently been found at circuit (14), cellular (11), and molecular levels (17–19). Anatomical studies provide evidence for similar connectivity among superficial, intermediate, and deep processing regions in avian A1 and the corresponding neocortical layers (11, 14, 15, 20, 21). For example, avian A1 is organized into columns of radially arranged intrinsic connections spanning all regions, similar to columns connecting neocortical layers (14). Further, the same genetically identified neuron types are found in intermediate, superficial, and deep neocortical layers and in distinct regions of avian A1 (17, 18).

Mammalian neocortical layers and the characteristic connections among layers define a "canonical" cortical microcircuit that is thought to underlie the computations required for complex cognition and behavior (22). Based on recent demonstrations of significant cognitive skills in birds and parallels in anatomical circuitry between the avian and mammalian cortex, we hypothesized that avian A1 exhibits the single neuron and population coding principles that characterize the canonical cortical microcircuit in the mammalian neocortex. By simultaneously recording the activity of 2–38 single neurons in each processing region of avian A1 and analyzing firing properties, we found that the avian cortex shows the hallmark information-processing features of the canonical cortical microcircuit, providing functional evidence for a common cortical microcircuit in mammals and birds. The information processing similarities described here suggest that birds and mammals have homologous cortical microcircuits and provide a physiological explanation for the evolution of neuronal processes that give rise to complex behavior in the absence of lamination.

Results

Hierarchical Processing in the Avian Auditory Cortex. A defining feature of the mammalian neocortical microcircuit is mainly feedforward connections that form a hierarchy of information-processing

Significance

A six-layered neocortex is a hallmark feature of the mammalian brain. Connections among layers and progressive changes in the neural coding properties of each layer define a microcircuit thought to perform the computations underlying complex behavior. Birds lack a six-layered cortex. Yet, they demonstrate complex cognition and behavior. Recent anatomical studies propose that adjacent regions of the avian pallium are homologs of neocortical layers. Here, we show that the avian auditory pallium exhibits the same information-processing principles that define the mammalian neocortical microcircuit. Results suggest that the cortical microcircuit evolved in a common ancestor of mammals and birds and provide a physiological explanation for neural processes that give rise to complex behavior in the absence of cortical lamination.

Author contributions: A.C. and S.M.N.W. designed research; A.C. performed research; A.C. analyzed data; A.C. and S.M.N.W. wrote the paper; and S.M.N.W. supervised the project.

The authors declare no conflict of interest.

This article is a PNAS Direct Submission. H.K. is a guest editor invited by the Editorial Board.

See Commentary on page 3184.

[1]To whom correspondence should be addressed. Email: sw2277@columbia.edu.

This article contains supporting information online at www.pnas.org/lookup/suppl/doi:10.1073/pnas.1408545112/-/DCSupplemental.

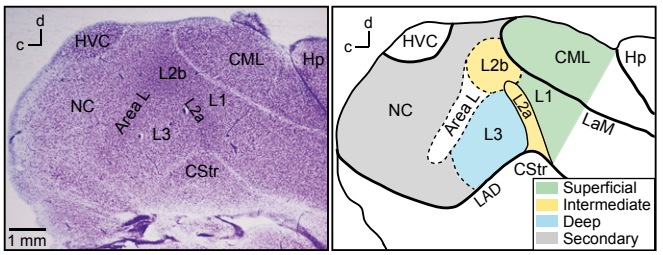

Fig. 1. Regions of the songbird auditory cortex. (*Left*) Nissl-stained parasagittal section showing cell bodies and laminae. (*Right*) Drawing of the same section with regions colored and labeled. Dashed lines indicate boundaries that are defined by transitions in cytoarchitecture. Field L regions L1, L2, L3, and lateral caudal mesopallium (CM) form the primary auditory cortex in birds (13, 14). Field L2a and L2b are the intermediate (thalamorecipient) regions. Field L1 and CML are the superficial regions, and field L3 is the deep region. Caudal nidopallium (NC) is a secondary auditory area. Area L (13) has cytoarchitecture similar to L2b but is not known to receive thalamic input. CStr, caudal striatum; Hp, hippocampus; HVC, (proper name) a song system premotor nucleus; LAD, lamina arcopallialis dorsalis; LaM, lamina mesopallialis.

stages. Sensory information from the thalamus largely targets the intermediate layer 4 and sparsely targets the layer 5/6 border (23, 24). From layer 4, axonal projections go to the superficial layers 2/3 and then to the deep layers 5/6, where information is distributed to other cortical and subcortical targets (23, 25). In primary auditory (A1), visual (V1), and somatosensory (S1) cortices, receptive fields are simple and separable in layer 4 and more complex and nonlinear in superficial and deep layers (26–29). Sensory evoked responses are generally sparser and more selective in layers downstream of layer 4 (30–32) although firing rates in layers 4 and 5 are similar in some systems (30, 33, 34).

As in mammalian sensory cortex, thalamic projections to avian A1 terminate mainly in the intermediate region and sparsely in the deep region (15, 20) (Fig. 2*A*). Information from the intermediate region field L2 is distributed to the superficial regions (field L1 and CML) and the deep region field L3 (14, 15, 20). To test whether hierarchical information processing is a main feature of the avian auditory microcircuit, we used multielectrode arrays to simultaneously record auditory responses from single neurons in the intermediate (n = 94), superficial (n = 219), and deep (n = 237) regions of avian A1, in unanesthetized adult male zebra finches (n = 6) (Fig. 2, Figs. S1 and S2, and Table S1). We also recorded from the secondary auditory cortex region NC (n = 273), which receives input from the deep and superficial regions of avian A1 (15, 20).

We found that the avian auditory cortex shows the hierarchical information-processing features that characterize the mammalian neocortex (Fig. 2). Response latencies to presentation of modulation-limited (ml) noise (correlated Gaussian noise matching zebra finch song in frequency range and maximum spectral and temporal modulation frequencies) (35) (*Materials and Methods*) were shortest in the intermediate region and significantly longer in the superficial and secondary regions (Fig. 2*A*) ($P < 0.05$, Kruskal–Wallis test with multiple comparisons correction). Fig. 2*C* shows spike trains recorded from single neurons in each region before, during, and after the presentation of ml noise, and the receptive fields (*SI Materials and Methods*) for those neurons. Single-cell sparseness, measured as sound-evoked firing rates, and population sparseness, computed as the fraction of cells that failed to produce a significant response to each presented stimulus (*SI Materials and Methods*), differed across regions; activity was densest in the intermediate region and significantly sparser in the superficial, deep, and secondary regions ($P < 0.05$) (Fig. 2 *D* and *E*). Stimulus selectivity (the fraction of stimuli that did not evoke a significant response from a neuron) was lowest in the intermediate region and significantly higher at successive processing stages ($P < 0.05$, Fig. 2*F*). Receptive field (RF) separability and linearity, two measures of RF simplicity (*SI Materials and Methods*), were highest in the intermediate region, lower in the superficial region, still lower in the deep region, and lowest in secondary cortex (Fig. 2 *G* and *H*) ($P < 0.05$). These results agree with analyses of sensory processing in the mammalian neocortex (26–28, 31, 32) and provide evidence that hierarchical information processing is also a defining feature of the avian auditory microcircuit. We found one difference in comparisons of processing between the avian and

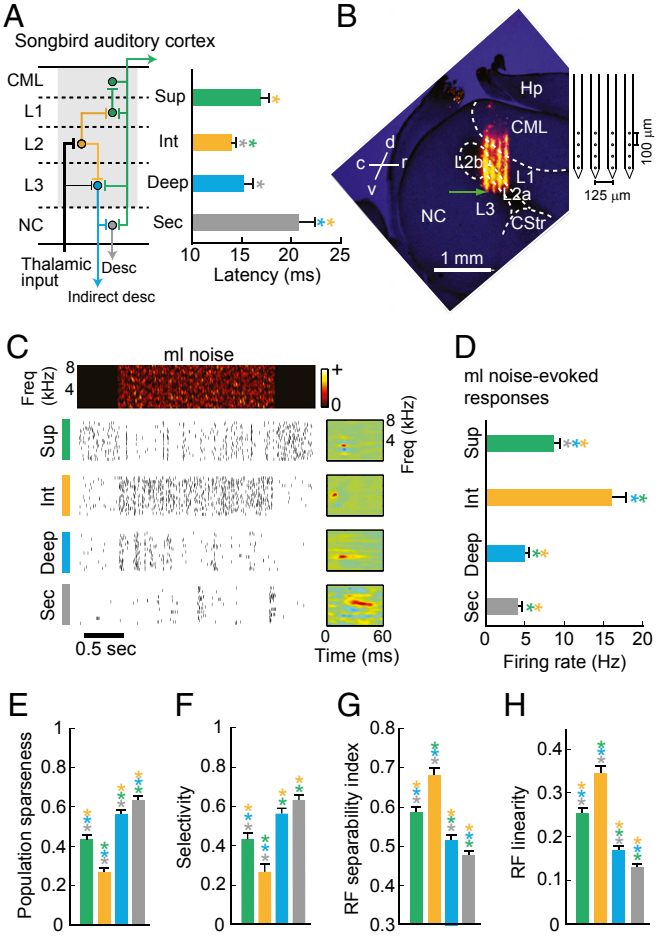

Fig. 2. Hierarchical information processing in the songbird auditory cortex. (*A*, *Left*) Schematic of the major projections in the songbird auditory cortex (modified from ref. 16). Shaded area indicates the circuitry corresponding to the mammalian primary auditory cortex. Thalamic input terminates largely in field L2 (intermediate region) and sparsely in field L3 (deep region). Dorsal projections from L2 terminate in L1, and L1 projects to CML (superficial regions). Ventral projections from L2 terminate in L3. Field L3 projects to NC (secondary), thalamus, and brainstem. (*Right*) Mean response latencies in different regions of the auditory microcircuit and secondary region NC. Latencies are shortest in the intermediate region and significantly longer in superficial and secondary regions. (*B*, *Left*) Histological image used to determine the polytrode location of one recording penetration. Four orange tracks show the locations of the four DiI–labeled polytrode shanks. The green arrow indicates the inferred location of the electrode shank tip. (*Right*) Polytrode schematic. (*C*) Example spike trains and receptive fields (RFs) of single neurons in superficial, intermediate, deep, and secondary regions. A spectrogram of the stimulus (2 s of ml noise) is shown above the spike trains. (*D*) Evoked firing rates (single-cell sparseness). (*E*) Population sparseness. (*F*) Selectivity. (*G*) RF separability index. (*H*) RF linearity. In bar graphs, error bars indicate SEM. Asterisks are color-coded according to region and indicate significant comparisons ($P < 0.05$, Kruskal–Wallis test with multiple groups comparison correction).

mammalian cortical microcircuits. Studies in A1 and S1 show that activity is sparser and more selective in superficial layers than in deep layers (28, 30). We found that sparseness and selectivity were higher in deep avian A1 than in superficial A1 (Fig. 2 *C–E*). This observation is consistent with recent findings (36) in the European starling and may be a microcircuit difference between birds and mammals.

Two Major Classes of Neurons in the Avian Auditory Cortex. A defining characteristic of the mammalian neocortex is the presence of two major classes of neurons. Excitatory principal cells (PCs) fire broad (also called wide or regular) action potentials at relatively low rates, and inhibitory interneurons (INs) fire narrow (i.e., thin or fast) action potentials at higher rates (23, 25, 37). PCs produce heterogeneous, comparatively sparse, and selective sensory responses whereas INs respond to the same stimuli with lower sparseness and selectivity, resulting in dense sensory representations (30, 38–40). In mammalian A1, PCs and INs also differ in RF structure; PCs have more complex RFs than do INs (41). To test whether avian A1 neurons group into two main classes, we subjected all recorded cells (n = 823) to a cluster analysis based on action potential (AP) shape (30, 36, 37) (Fig. 3*A*, Fig. S3, and *SI Materials and Methods*). Neurons clustered into two classes, and both classes were found in superficial, intermediate, and deep regions, as well as in the secondary auditory cortex (Fig. 3*B* and Figs. S3 and S4). Action potentials of putative INs (pINs, n = 235/823) were significantly narrower (0.33 ± 0.05 ms) than those of putative PCs (pPCs, n = 588/823) (0.77 ± 0.13 ms) (P < 1e−10, two-sample Kolmogorov–Smirnov test). As in the neocortex (38), firing rate and AP width were negatively correlated; neurons with higher firing rates generally had narrower APs (Pearson's correlation coefficient (R) = −0.58) (Fig. 3*A* and Fig. S3). Fig. 3*B* shows example spike trains and RFs of pINs and pPCs in each region. As in the mammalian neocortex (30, 38, 39), pPCs had more heterogeneous responses and RF structures than did pINs, within and across regions (Fig. 3). Fig. S5 shows pPC spike trains and RFs, organized by AP width. Like neocortical INs and PCs within a layer, avian pPCs exhibited lower evoked firing rates and higher stimulus selectivity than did pINs in the same region (Fig. 3 *C–E*, compare blue and red in each panel, P < 0.01 two-sample Kolmogorov–Smirnov test). Also as in neocortex, the RFs of pPCs were less linear and more complex than were the RFs of pINs (Fig. 3 *F* and *G*). Response properties and RF structures of pINs and pPCs also differed across regions. Broadly following the hierarchical organization shown in Fig. 2, response sparseness (Fig. 3 *C* and *D*) selectivity (Fig. 3*E*), and RF complexity (Fig. 3 *F* and *G*) increased in successive processing stages beyond the thalamorecipient region, in both pPCs and pINs (compare bars of the same color in each panel). Results indicate that differences in single neuron coding properties across processing regions and between neuron classes are similar in the avian and mammalian primary cortex.

Population Coding Differences Across Regions, Neuron Types, and Anatomical Distance. Neuronal populations in the neocortex show distinct patterns of connectivity in different layers and between neuron classes (e.g., PC or IN) in the population. Correlations in the timing of spikes produced by different neurons reflect the strength and specificity of connections among neurons in a population and are measured as spike-count correlations between simultaneously recorded neurons. Stimulus-evoked and spontaneous noise correlations (those due to shared input or direct synaptic connections) differ across layers and in populations of PCs and INs depending on the connectivity patterns in each layer and neuron class (23, 31, 42, 43). First, the connectivity in thalamorecipient layer 4 is local and homogenous (44), and single neurons have diverse firing properties (43, 45, 46). These characteristics are consistent with the observation of weak pairwise correlations in layer 4 compared with those in superficial and deep layers (31, 43). In contrast to layer 4, neurons in deep output layers have long-range, recurrent connections and strong noise correlations (43, 46). Second, pairwise correlations differ in populations of PCs and

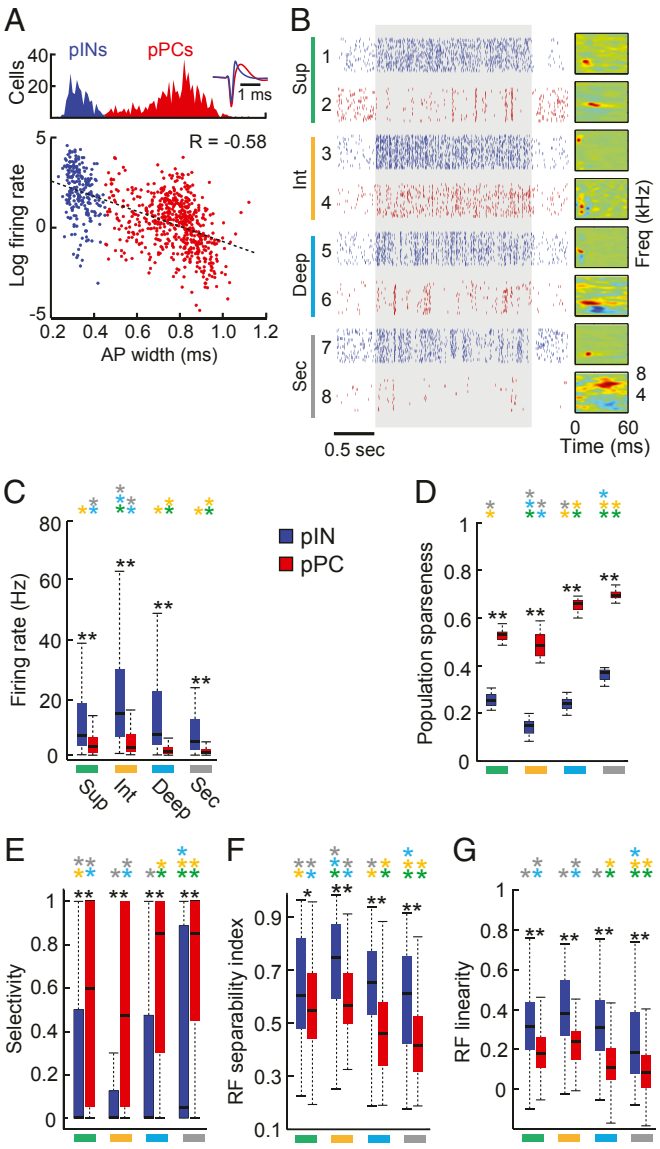

Fig. 3. Response properties of pPCs and pINs in the songbird auditory cortex. (*A*) Identification of putative principal cells (pPCs, n = 588) and putative fast-spiking interneurons (pINs, n = 235) by spike waveform shape. Spike-sorted units were classified based on mean spike waveform width and grouped into two classes using a Gaussian mixture model (Fig. S3). Putative INs (blue) have narrow spike waveforms whereas pPCs (red) have wider spikes. Action potential width is negatively correlated with evoked firing rate; firing rates are higher in neurons with narrower spikes (n = 823 neurons), Pearson's correlation coefficient, R = −0.58. (*B*) Spike train responses to 30 repetitions of ml noise for eight example neurons. Neurons 1, 3, 5, and 7 are pINs (blue). Neurons 2, 4, 6, and 8 are pPCs (red). The shaded area denotes the period of stimulus presentation. Receptive fields (RFs) for each example neuron are to the right of the raster plots. (*C*) Box plots of evoked firing rates for pINs (blue) and pPCs (red) shown by region. (*D*) Population sparseness. (*E*) Selectivity. (*F*) RF separability. (*G*) RF linearity. Black asterisks indicate significant differences between pPCs and pINs within a region (**P < 0.01; *P < 0.05; two-sample Kolmogorov–Smirnov test). Colored asterisks indicate significant differences among regions for pINs and pPCs separately (P < 0.05, Kruskal–Wallis test with multiple groups comparison correction).

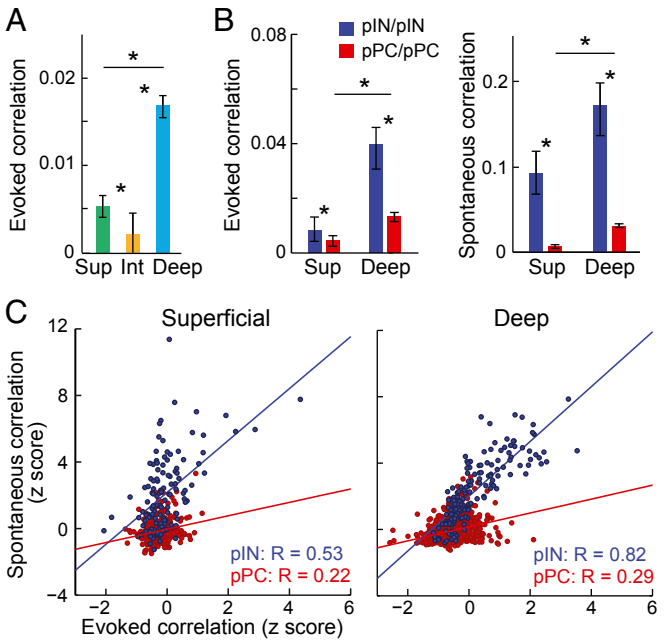

Fig. 4. Noise correlations by region and neuron type. (*A*) Pairwise noise correlations during evoked activity for superficial, intermediate, and deep regions. Asterisks indicate significant differences in correlations between regions ($P < 0.05$, Kruskal–Wallis test with multiple groups comparison correction). Bars represent population medians, and error bars indicate 95% confidence intervals for the medians. (*B*) Pairwise correlations for pINs and pPCs in superficial and deep regions for evoked (*Left*) and spontaneous (*Right*) activity. Note that *y* axes are on different scales in *Left* and *Right* panels. (*C*) Relationships between normalized (z-scored) spontaneous and evoked correlations in pIN pairs (blue) and pPC pairs (red), in the superficial (*Left*) and deep (*Right*) regions. In both superficial and deep regions, evoked correlations scaled with spontaneous correlations for pairs of pINs but not for pairs of pPCs. Plots show spontaneous pairwise correlations by evoked pairwise correlations. Each point represents one pair. Pearson's correlation coefficients (R) quantifying the relationship between spontaneous and evoked correlations for pIN/pIN and pPC/pPC pairs are shown in the bottom right corner of each plot. Red and blue lines correspond to linear fits to the data.

INs; correlations between fast-spiking INs are stronger than those between PCs in both superficial and deep layers, consistent with the denser and more widespread connectivity among INs than among PCs (30, 42, 47). Additionally, the sparse responses and localized connectivity in superficial-layer PCs compared with deep PCs underlie the weaker correlations between PCs in superficial layers compared with those in deep layers (30, 42, 48). Third, the density of connections among neurons in a population impacts how much sensory stimulation controls population activity; pairwise correlations in evoked and spontaneous activity are significantly more similar in heavily interconnected populations of INs than in populations of PCs with sparser connectivity (23, 42). Fourth, correlations in evoked and spontaneous activity vary with anatomical distance based on the spatial extent of connectivity. Connections among neurons are more localized in superficial layers than in deep layers, providing an anatomical basis for the dependence of pairwise correlation strength on spatial distance between neurons in superficial, but not in deep, populations (30). Excitatory connections in superficial layers significantly decay as distances between neurons approach 150 μm (49, 50) whereas excitatory connections in deep layers are typically widespread (47, 49–52). These structural differences support local clustering of spiking activity in superficial layers and larger spreads of correlated firing in deep layers.

To test whether avian A1 shows population-coding differences across regions, neuron classes, and anatomical distances that map onto those in the neocortex, we compared evoked and spontaneous pairwise correlations in (*i*) intermediate, superficial, and deep regions (Fig. 4 and Fig. S6), (*ii*) pPCs and pINs (Figs. 4 and 5 and Fig. S6), (*iii*) superficial and deep pPCs (Fig. 4*B*), and (*iv*) pairs with short and long interneuron spatial distances (Fig. 5). We

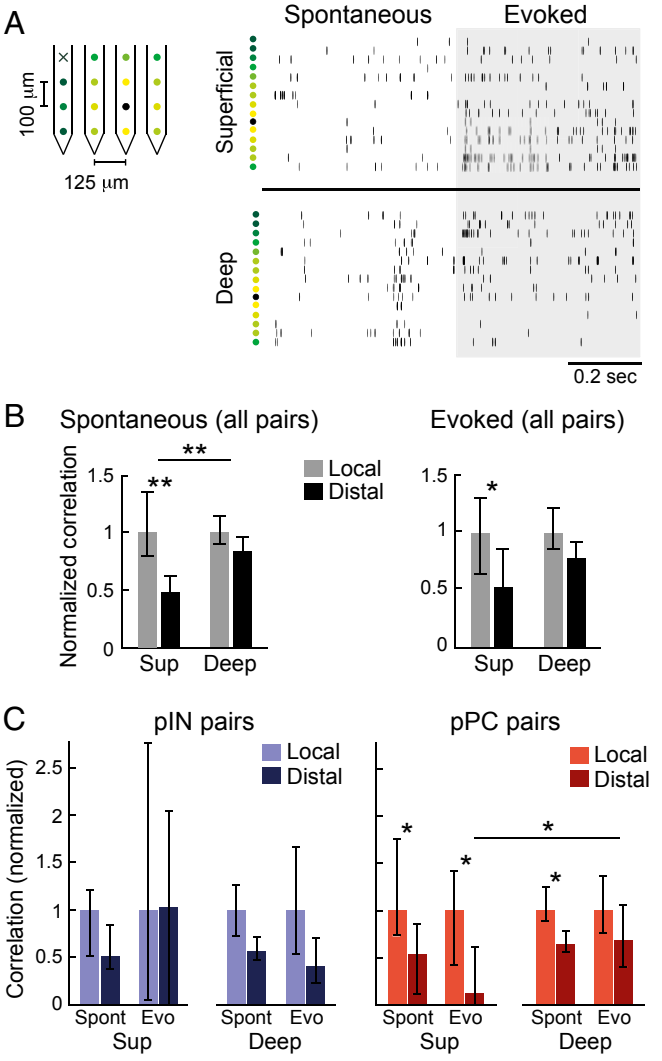

Fig. 5. Relationship between pairwise correlations and anatomical distance by region and neuron type. (*A*) Example of simultaneous recordings of multiunit (non–spike-sorted) activity from multiple electrode contacts, in the superficial (*Top Right*) and deep (*Bottom Right*) regions. Rasters are organized by increasing distance from the black recording contact. Colored dots to the left of rasters correspond to colors labeling recording contacts on the polytrode (*Left*). Black "x" indicates a nonfunctional contact. (*B*) Spatial dependence of normalized noise correlations in superficial and deep regions for spontaneous (*Left*) and evoked (*Right*) activity. Local pairs were those in which recorded neurons were ≤150 μm apart. Distal pairs were those in which recorded neurons were ≥300 μm apart. Pairwise correlations in each region were normalized by dividing by the median of the local correlations in that region to place correlations in all regions on the same scale, allowing comparison of correlations between regions. Bars show population medians, and error bars show 95% confidence intervals. Asterisks indicate significant comparisons (Kruskal–Wallis test with multiple groups comparison correction, $*P < 0.05$, $**P < 0.01$). Correlations in the superficial region decayed with anatomical distance more than did correlations in the deep region. (*C*) As in *B*, but with correlations for pairs of pINs and pairs of pPCs shown separately.

computed pairwise spike-count correlations between all simultaneously recorded neurons in each region (Figs. S1 and S2 and *SI Materials and Methods*) and found that population-coding differences in regions, in neuron classes, and across spatial distance were strikingly similar to those in neocortex. First, as in mammals, overall noise correlations (all pairs combined) in evoked activity were weak in the intermediate region and stronger in superficial and deep regions (Fig. 4*A*) ($P < 0.05$, Kruskal–Wallis test with multiple comparisons correction). Second, evoked and spontaneous correlations between pairs of pPCs were significantly weaker than between pairs of pINs, supporting the prevailing inference that INs are more densely connected than are PCs (Fig. 4*B*) ($P < 0.05$, Kruskal–Wallis test with multiple comparisons correction; Fig. S6 shows pPC/pIN pairs). Correlations in pPC/pPC pairs were also stronger in the deep region than in the superficial region (Fig. 4*B*, $P < 0.05$, compare red bars in each panel). These results are physiological evidence that, like in neocortex, deep pPCs are more heavily interconnected than are superficial pPCs. Third, correlations in spontaneous activity were stronger than correlations in evoked activity in all regions (compare scales in Fig. 4*B*), indicating that stimulus drive decorrelates population firing in both birds and mammals (30, 53). We also found a stronger relationship between spontaneous and evoked correlations in pIN pairs than in pPC pairs, in both superficial and deep regions, providing further evidence that connectivity is denser among INs than among PCs in birds as in mammals (Fig. 4*C*, compare red and blue points in each panel; for superficial pairs, R_{IN}, $P = 3.55e{-}10$ and R_{PC}, $P = 8.1e{-}06$; for deep pairs, R_{IN}, $P = 1.86e{-}38$ and R_{PC}, $P = 1.35e{-}20$). Fig. S6 shows intermediate region correlations, and Table S2 shows median correlation strengths for each region and neuron class, measured from evoked and spontaneous activity separately. Fourth, we found that correlation strength depended on the spatial distance between recorded neurons significantly more in superficial than in deep populations (Fig. 5 and *SI Materials and Methods*). Raster plots of multiunit (non–spike-sorted) activity in Fig. 5*A* show similar spiking activity across recording contacts in the deep region but not in the superficial region, suggesting longer range connectivity among deep-region neurons. In spontaneous activity, correlations between superficial neurons were significantly weaker in pairs of "distal" (≥300 μm apart) neurons than in pairs of "local" (≤150 μm apart) neurons (Fig. 5 *B* and *C*) ($P < 0.01$). Correlations in the deep region did not decrease with anatomical distance, matching findings in mammalian A1 (30). Correlation strength in evoked activity also decreased with distance in the superior but not deep region (Fig. 5*B*, *Right*) ($P < 0.05$). Correlations computed for pPC pairs and pIN pairs separately showed that correlations did not decrease with anatomical distance in pIN pairs (Fig. 5*C*, *Left*) and that correlations in pPC pairs decreased with anatomical distance more in the superficial than in the deep region (Fig. 5*C*, *Right*) ($P < 0.05$, Kruskal–Wallis test with multiple comparisons correction). These analyses demonstrate that the properties of correlated activity in the processing regions and neuron classes of the avian auditory cortex closely match those reported for corresponding layers and neuron classes in the mammalian neocortex.

Discussion

Analyses of single neuron and population activity in and across all regions of the avian auditory cortex indicate that the information-coding properties of avian A1 are highly similar to those that define the "canonical cortical microcircuit" in mammals. First, adjacent and connected regions of the avian auditory cortex form a hierarchy of information processing. Second, the same two classes of neurons are found in the mammalian and avian cortex. Third, neurons in the neocortex and avian cortex exhibit comparable single-cell and population-coding strategies across cortical regions/layers, between neuron types, and over anatomical distance. The similarity between these findings and what is known about sensory processing in the mammalian neocortex supports the homology hypothesis of brain evolution (54) and suggests that the canonical cortical microcircuit evolved in a common ancestor of mammals and birds (11, 14, 17). If so, then the microcircuit evolved in stem amniotes and predates cortical lamination by at least 100 million y (12). An alternative possibility is that pallium evolution in birds and mammals converged on the same circuit organization for information processing (11). Regardless of these alternatives, this study provides a physiological explanation for the evolution of neural processes that give rise to complex behavior in the absence of lamination.

Materials and Methods

Full methods are provided in *SI Materials and Methods*.

Groups of auditory neurons were recorded in the superficial ($n = 219$), intermediate ($n = 94$), and deep ($n = 237$) regions of the primary auditory cortex of six head-restrained, unanesthetized, male zebra finches (Table S1). All procedures involving animals were reviewed and approved by the Columbia University Institutional Animal Care and Use Committee. Recordings were made from the same birds in the caudal nidopallium (NC), a secondary auditory cortical region ($n = 273$). Neural responses were evoked by presentation of 10 distinct samples (each = 2 s duration) of modulation-limited (ml) noise. Ml noise is correlated Gaussian noise filtered to match the frequency range (250–8,000 Hz) and maximum spectral and temporal modulation frequencies of zebra finch song (35, 55). Each of the 10 stimuli was presented 30–40 times in pseudorandom order. Data analysis was carried out in MATLAB (Mathworks). Spikes were sorted offline (56–59). All recorded single units ($n = 823$) were classified as putative interneurons (pINs) or putative principal cells (pPCs) based on action potential width (Fig. 3 and Fig. S3). For each processing region and each neuron class, single-cell sparseness was computed as the sound-evoked firing rate. Population sparseness was computed as the fraction of cells that did not produce a significant response to a given stimulus. Selectivity was computed as the fraction of different stimuli that did not elicit a significant response from a given neuron. Spectrotemporal receptive fields (STRFs) were computed by fitting a generalized linear model to the sound-evoked responses of each neuron (60). The response latency for each neuron was computed from the STRF, at the best excitatory frequency (61) (*SI Materials and Methods*). Receptive field separability was computed by performing a singular value decomposition on the STRF. Receptive field linearity was measured by using the STRF to predict responses to novel stimuli. Spontaneous and evoked spike-count correlations were obtained by computing Pearson's correlation coefficient between spike counts (50-ms sliding window) from the spike trains of all simultaneously recorded neurons (excluding pairs recorded from the same electrode contact). Noise correlations were measured using a shift predictor to correct for stimulus-induced correlations (53, 62). In Fig. 5 *B* and *C*, pairwise correlations in a region were normalized by dividing by the median of the local correlations in that region so that correlations in all regions were on the same scale, allowing the comparison of correlations in superficial and deep regions.

ACKNOWLEDGMENTS. We thank J. Moore and J. Schumacher for comments on the manuscript and for their input on experimental design and data analysis and R. Bruno and S. Rosis for comments on the manuscript. A.C. was supported by a Howard Hughes Medical Institute International Predoctoral Fellowship, and S.M.N.W. was supported by NIH Grant R01-DC009810.

1. Weir AA, Chappell J, Kacelnik A (2002) Shaping of hooks in New Caledonian crows. *Science* 297(5583):981.
2. Pika S, Bugnyar T (2011) The use of referential gestures in ravens (Corvus corax) in the wild. *Nat Commun* 2:560.
3. Taylor AH, Miller R, Gray RD (2012) New Caledonian crows reason about hidden causal agents. *Proc Natl Acad Sci USA* 109(40):16389–16391.
4. Veit L, Nieder A (2013) Abstract rule neurons in the endbrain support intelligent behaviour in corvid songbirds. *Nat Commun* 4:2878.
5. Prior H, Schwarz A, Güntürkün O (2008) Mirror-induced behavior in the magpie (Pica pica): Evidence of self-recognition. *PLoS Biol* 6(8):e202.
6. Raby CR, Alexis DM, Dickinson A, Clayton NS (2007) Planning for the future by western scrub-jays. *Nature* 445(7130):919–921.

7. Yamazaki Y, Aust U, Huber L, Hausmann M, Güntürkün O (2007) Lateralized cognition: Asymmetrical and complementary strategies of pigeons during discrimination of the "human concept". *Cognition* 104(2):315–344.
8. Fagot J, Cook RG (2006) Evidence for large long-term memory capacities in baboons and pigeons and its implications for learning and the evolution of cognition. *Proc Natl Acad Sci USA* 103(46):17564–17567.
9. Scarf D, Hayne H, Colombo M (2011) Pigeons on par with primates in numerical competence. *Science* 334(6063):1664.
10. Brainard MS, Doupe AJ (2013) Translating birdsong: Songbirds as a model for basic and applied medical research. *Annu Rev Neurosci* 36:489–517.
11. Reiner A, Yamamoto K, Karten HJ (2005) Organization and evolution of the avian forebrain. *Anat Rec A Discov Mol Cell Evol Biol* 287(1):1080–1102.
12. Jarvis ED, et al.; Avian Brain Nomenclature Consortium (2005) Avian brains and a new understanding of vertebrate brain evolution. *Nat Rev Neurosci* 6(2):151–159.
13. Fortune ES, Margoliash D (1992) Cytoarchitectonic organization and morphology of cells of the field L complex in male zebra finches (Taenopygia guttata). *J Comp Neurol* 325(3):388–404.
14. Wang Y, Brzozowska-Prechtl A, Karten HJ (2010) Laminar and columnar auditory cortex in avian brain. *Proc Natl Acad Sci USA* 107(28):12676–12681.
15. Vates GE, Broome BM, Mello CV, Nottebohm F (1996) Auditory pathways of caudal telencephalon and their relation to the song system of adult male zebra finches. *J Comp Neurol* 366(4):613–642.
16. Karten HJ (2013) Neocortical evolution: Neuronal circuits arise independently of lamination. *Curr Biol* 23(1):R12–R15.
17. Dugas-Ford J, Rowell JJ, Ragsdale CW (2012) Cell-type homologies and the origins of the neocortex. *Proc Natl Acad Sci USA* 109(42):16974–16979.
18. Suzuki IK, Kawasaki T, Gojobori T, Hirata T (2012) The temporal sequence of the mammalian neocortical neurogenetic program drives mediolateral pattern in the chick pallium. *Dev Cell* 22(4):863–870.
19. Atoji Y, Karim MR (2014) Expression of vesicular glutamate transporter 3 mRNA in the brain and retina of the pigeon. *J Chem Neuroanat* 61-62:124–131.
20. Wild JM, Karten HJ, Frost BJ (1993) Connections of the auditory forebrain in the pigeon (Columba livia). *J Comp Neurol* 337(1):32–62.
21. Zeng S, Zhang X, Peng W, Zuo M (2004) Immunohistochemistry and neural connectivity of the Ov shell in the songbird and their evolutionary implications. *J Comp Neurol* 470(2):192–209.
22. Dunbar RIM (1998) The social brain hypothesis. *Evol Anthropol* 6(5):178–190.
23. Harris KD, Mrsic-Flogel TD (2013) Cortical connectivity and sensory coding. *Nature* 503(7474):51–58.
24. Constantinople CM, Bruno RM (2013) Deep cortical layers are activated directly by thalamus. *Science* 340(6140):1591–1594.
25. Douglas RJ, Martin KA (2004) Neuronal circuits of the neocortex. *Annu Rev Neurosci* 27:419–451.
26. Gilbert CD, Wiesel TN (1979) Morphology and intracortical projections of functionally characterised neurones in the cat visual cortex. *Nature* 280(5718):120–125.
27. Martinez LM, et al. (2005) Receptive field structure varies with layer in the primary visual cortex. *Nat Neurosci* 8(3):372–379.
28. Atencio CA, Sharpee TO, Schreiner CE (2009) Hierarchical computation in the canonical auditory cortical circuit. *Proc Natl Acad Sci USA* 106(51):21894–21899.
29. Brumberg JC, Pinto DJ, Simons DJ (1999) Cortical columnar processing in the rat whisker-to-barrel system. *J Neurophysiol* 82(4):1808–1817.
30. Sakata S, Harris KD (2009) Laminar structure of spontaneous and sensory-evoked population activity in auditory cortex. *Neuron* 64(3):404–418.
31. Smith MA, Jia X, Zandvakili A, Kohn A (2013) Laminar dependence of neuronal correlations in visual cortex. *J Neurophysiol* 109(4):940–947.
32. Wright N, Fox K (2010) Origins of cortical layer V surround receptive fields in the rat barrel cortex. *J Neurophysiol* 103(2):709–724.
33. O'Connor DH, Peron SP, Huber D, Svoboda K (2010) Neural activity in barrel cortex underlying vibrissa-based object localization in mice. *Neuron* 67(6):1048–1061.
34. Manns ID, Sakmann B, Brecht M (2004) Sub- and suprathreshold receptive field properties of pyramidal neurones in layers 5A and 5B of rat somatosensory barrel cortex. *J Physiol* 556(Pt 2):601–622.
35. Schneider DM, Woolley SM (2011) Extra-classical tuning predicts stimulus-dependent receptive fields in auditory neurons. *J Neurosci* 31(33):11867–11878.
36. Meliza CD, Margoliash D (2012) Emergence of selectivity and tolerance in the avian auditory cortex. *J Neurosci* 32(43):15158–15168.
37. Barthó P, et al. (2004) Characterization of neocortical principal cells and interneurons by network interactions and extracellular features. *J Neurophysiol* 92(1):600–608.
38. Hromádka T, Deweese MR, Zador AM (2008) Sparse representation of sounds in the unanesthetized auditory cortex. *PLoS Biol* 6(1):e16.
39. Cardin JA, Palmer LA, Contreras D (2007) Stimulus feature selectivity in excitatory and inhibitory neurons in primary visual cortex. *J Neurosci* 27(39):10333–10344.
40. Bruno RM, Simons DJ (2002) Feedforward mechanisms of excitatory and inhibitory cortical receptive fields. *J Neurosci* 22(24):10966–10975.
41. Atencio CA, Schreiner CE (2008) Spectrotemporal processing differences between auditory cortical fast-spiking and regular-spiking neurons. *J Neurosci* 28(15):3897–3910.
42. Hofer SB, et al. (2011) Differential connectivity and response dynamics of excitatory and inhibitory neurons in visual cortex. *Nat Neurosci* 14(8):1045–1052.
43. Hansen BJ, Chelaru MI, Dragoi V (2012) Correlated variability in laminar cortical circuits. *Neuron* 76(3):590–602.
44. Blasdel GG, Lund JS (1983) Termination of afferent axons in macaque striate cortex. *J Neurosci* 3(7):1389–1413.
45. Renart A, et al. (2010) The asynchronous state in cortical circuits. *Science* 327(5965): 587–590.
46. Litwin-Kumar A, Doiron B (2012) Slow dynamics and high variability in balanced cortical networks with clustered connections. *Nat Neurosci* 15(11):1498–1505.
47. Thomson AM, Lamy C (2007) Functional maps of neocortical local circuitry. *Front Neurosci* 1(1):19–42.
48. Ko H, et al. (2011) Functional specificity of local synaptic connections in neocortical networks. *Nature* 473(7345):87–91.
49. Holmgren C, Harkany T, Svennenfors B, Zilberter Y (2003) Pyramidal cell communication within local networks in layer 2/3 of rat neocortex. *J Physiol* 551(Pt 1):139–153.
50. Oswald AM, Reyes AD (2008) Maturation of intrinsic and synaptic properties of layer 2/3 pyramidal neurons in mouse auditory cortex. *J Neurophysiol* 99(6):2998–3008.
51. Schubert D, Kötter R, Staiger JF (2007) Mapping functional connectivity in barrel-related columns reveals layer- and cell type-specific microcircuits. *Brain Struct Funct* 212(2):107–119.
52. Feldmeyer D, Lübke J, Sakmann B (2006) Efficacy and connectivity of intracolumnar pairs of layer 2/3 pyramidal cells in the barrel cortex of juvenile rats. *J Physiol* 575(Pt 2): 583–602.
53. Kohn A, Smith MA (2005) Stimulus dependence of neuronal correlation in primary visual cortex of the macaque. *J Neurosci* 25(14):3661–3673.
54. Karten HJ (1969) Organization of avian telencephalon and some speculations on phylogeny of amniote telencephalon. *Ann N Y Acad Sci* 167(A1):164–179.
55. Woolley SM, Fremouw TE, Hsu A, Theunissen FE (2005) Tuning for spectro-temporal modulations as a mechanism for auditory discrimination of natural sounds. *Nat Neurosci* 8(10):1371–1379.
56. Kim KH, Kim SJ (2000) Neural spike sorting under nearly 0-dB signal-to-noise ratio using nonlinear energy operator and artificial neural-network classifier. *IEEE Trans Biomed Eng* 47(10):1406–1411.
57. Quiroga RQ, Nadasdy Z, Ben-Shaul Y (2004) Unsupervised spike detection and sorting with wavelets and superparamagnetic clustering. *Neural Comput* 16(8):1661–1687.
58. Kelly RC, et al. (2007) Comparison of recordings from microelectrode arrays and single electrodes in the visual cortex. *J Neurosci* 27(2):261–264.
59. Hill DN, Mehta SB, Kleinfeld D (2011) Quality metrics to accompany spike sorting of extracellular signals. *J Neurosci* 31(24):8699–8705.
60. Calabrese A, Schumacher JW, Schneider DM, Paninski L, Woolley SM (2011) A generalized linear model for estimating spectrotemporal receptive fields from responses to natural sounds. *PLoS ONE* 6(1):e16104.
61. Schumacher JW, Schneider DM, Woolley SM (2011) Anesthetic state modulates excitability but not spectral tuning or neural discrimination in single auditory midbrain neurons. *J Neurophysiol* 106(2):500–514.
62. Bair W, Zohary E, Newsome WT (2001) Correlated firing in macaque visual area MT: Time scales and relationship to behavior. *J Neurosci* 21(5):1676–1697.